Annals of Mathematical Sciences and Applications
Volume 8, Number 3, 547–563, 2023

A least-squares method for the numerical solution of a 2D optimal transportation problem*

Alexandre Caboussat and Dimitrios Gourzoulidis

In memory of Prof. Roland Glowinski

Optimal transportation of raw material from suppliers to customers is an issue in supply chain that we address here with a continuous model. A least-squares method is designed to solve the prescribed Jacobian problem that arises in optimal transportation in two dimensions of space. An iterative algorithm allows to decouple the variational aspects of the problem from the nonlinearities and from the weak treatment of the boundary conditions. Numerical experiments illustrate the transport of material in several configurations.

AMS 2000 subject classifications: 65N30, 65K10, 49M20, 35F30.
Keywords and phrases: Optimal transport, prescribed Jacobian equation, Monge-Ampère equation, least-squares method, mixed finite element method.

1. Introduction

Optimal transportation has raised many challenging mathematical problems in the literature [1, 17, 21]. It has also many applications in other communities, such as logistics and operations research, when considering the transport of raw material along a supply chain [14, 16]. When considering a continuous approach, modeling the optimal transport problem has led to strong links with, e.g., the Monge-Ampère equation [9, 11, 12] or the prescribed Jacobian equation [10].

Our underlying application of interest is the transport of food waste material from suppliers to a warehouse [5], which is commonly addressed with a discrete method [20] within the operational research community, typically using graph theory and linear and/or integer programming techniques. From a continuous viewpoint, optimal transport can be used to describe the physical transport of material from point A (source) to point B (destination). In

*Partially supported by HES-SO RCSO E&M project #118745.

the spirit of Monge [13], material has to be transported from suppliers (or sources) to destination points.

Using various models, many numerical methods have been proposed in the literature to approximate the solution to the optimal transport problem [16], ranging from finite differences approaches [2, 4] to finite element methods [3, 18, 22].

In this work, we extend the methodology presented in [6, 7] to solve a prescribed Jacobian equation for the optimal mapping, together with numerical methods designed when solving the 2D Monge-Ampère equation [8]. The main differences are the enforcement of so-called transport boundary conditions, and an original mix of numerical algorithms that are all tributes to Prof. R. Glowinski. The methodology relies on a least-squares approach and a relaxation algorithm of the ADMM type to decouple the variational aspects of the problem from the nonlinearities, which require mathematical programming approaches. The discretization method employs low order, piecewise linear, mixed finite elements. Numerical experiments illustrate the characteristics of the approach and show directions for future research.

2. Mathematical model

Let us describe first the optimal transport problem in the sense of Monge [13]. Let Ω be a bounded domain of $\mathbb{R}^2$ and $\mathcal{X}, \mathcal{Y} \subset \Omega$ two subdomains of Ω. Let $f : \mathcal{X} \to \mathbb{R}^2$ and $g : \mathcal{Y} \to \mathbb{R}^2$ be given (mass) densities. The optimal transport problem consists in moving these mass densities from $\mathcal{X}$ onto $\mathcal{Y}$ while minimizing transportation costs. The problem is thus to find a mapping $\mathbf{m} : \mathcal{X} \to \mathcal{Y}$ such that

$$f(x,y) = g(\mathbf{m}(x,y)) \left|\det \nabla \mathbf{m}(x,y)\right|, \tag{1}$$

where $\nabla \mathbf{m}$ denotes the gradient of the mapping $\mathbf{m}$, with condition

$$\mathbf{m}(\mathcal{X}) = \mathcal{Y}. \tag{2}$$

One constraint is that the total mass in $\mathcal{X}$ is equal to the total mass in $\mathcal{Y}$. This implies the following necessary condition

$$\int_{\mathcal{X}} f(x,y)dxdy = \int_{\mathcal{Y}} g(x,y)dxdy. \tag{3}$$

At the same time, we minimize the transportation cost $c = c(\mathbf{m})$ defined by

$$c(\mathbf{m}) = \int_{\mathcal{X}} \left|(x,y)^T - \mathbf{m}(x,y)\right|^2 f(x,y)dxdy. \tag{4}$$

It has been proved, see, e.g., [21], that there exists a mapping that satisfies (1) and minimizes (4). This mapping is the unique gradient of a convex function. It is also proved that the implicit condition (2) may be replaced by the following boundary condition

$$\mathbf{m}(\partial\mathcal{X}) = \partial\mathcal{Y}. \tag{5}$$

Figure 1 illustrates a sketch of the situation.

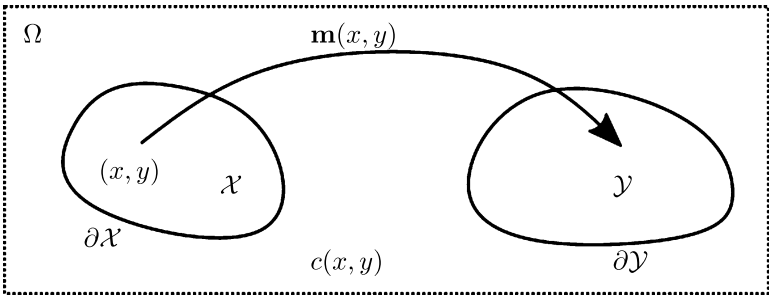

Figure 1: Sketch of the optimal transport problem mapping a domain $\mathcal{X}$ onto another domain $\mathcal{Y}$.

The underlying application is thus to transport a material from one place (suppliers) to another (customers) while minimizing the corresponding cost. The mathematical model we propose here relies on solving the prescribed Jacobian equation [10] with transport boundary condition, see, e.g., [18]. The partial differential equation involving the Jacobian determinant we want to solve reads as follows: find $\mathbf{m} : \mathcal{X} \to \mathcal{Y}$ satisfying

$$\begin{cases} \det \nabla \mathbf{m}(x,y) = \dfrac{f(x,y)}{g(\mathbf{m}(x,y))}, & \forall (x,y) \in \mathcal{X}, \\ \mathbf{m}(\partial\mathcal{X}) = \partial\mathcal{Y}. \end{cases} \tag{6}$$

A simpler problem has been investigated in [10] from a theoretical point of view, when considering Dirichlet boundary conditions with the identity function. The corresponding problem is of the following type

$$\begin{cases} \det \nabla \mathbf{m}(x,y) = f(x,y), & \forall (x,y) \in \mathcal{X}, \\ \mathbf{m}\,(x,y) = (x,y)^T, & a.e.\,(x,y) \in \partial\mathcal{X}. \end{cases}$$

A numerical method for the solution of this Dirichlet problem has been

proposed in [6, 7]. One of the objectives is to modify it to incorporate implicit transport boundary conditions such as those in (6).

3. Numerical method

3.1. Least-squares framework

We detail here the numerical method used to solve (6). Following [18], we extend the least-squares approach in [7] to account for the transport boundary conditions, and incorporate new algorithms into it. Let us define the following functional spaces

$$\begin{aligned}\mathbf{Q}(\mathbf{m}) &= \left\{ \mathbf{q} \in \left(L^2(\mathcal{X})\right)^{2\times 2},\ \mathbf{q} = \mathbf{q}^T,\ \det \mathbf{q} = \frac{f}{g(\mathbf{m})} \right\},\\ \mathbf{V} &= \left(H^1(\mathcal{X})\right)^2,\\ \mathcal{B} &= \left\{ \mathbf{b} \in \left(C(\partial\mathcal{X})\right)^2, \mathbf{b}(x,y) \in \partial\mathcal{Y} \right\}.\end{aligned}$$

Note that, unlike in [7], $\mathbf{Q}(\mathbf{m})$ includes only symmetric tensors since it has been proved that the optimal transportation map $\mathbf{m}$ is the gradient of a convex potential function. Let us introduce auxiliary variables $\mathbf{q} \in \mathbf{Q}(\mathbf{m})$ and $\mathbf{b} \in \mathcal{B}$ to decouple the variational aspects of the problem from the nonlinearities and from the implicit treatment of the boundary conditions.

Let $0 < \alpha < 1$ be a given parameter, and let us define the following functionals:

$$\begin{aligned}J_1(\mathbf{m},\mathbf{q}) &= \frac{1}{2}\int_{\mathcal{X}} \|\nabla\mathbf{m} - \mathbf{q}\|^2 dxdy;\\ J_2(\mathbf{m},\mathbf{b}) &= \frac{1}{2}\int_{\partial\mathcal{X}} |\mathbf{m} - \mathbf{b}|^2 ds;\\ J(\mathbf{m},\mathbf{q},\mathbf{b}) &= \alpha J_1(\mathbf{m},\mathbf{q}) + (1-\alpha) J_2(\mathbf{m},\mathbf{b}).\end{aligned}$$

The least-squares problem reads as follows: find $\{\mathbf{m},\mathbf{p},\mathbf{b}\} \in \mathbf{V} \times \mathbf{Q}(\mathbf{m}) \times \mathcal{B}$ such that

$$J(\mathbf{m},\mathbf{p},\mathbf{b}) \le J(\mathbf{u},\mathbf{q},\mathbf{a}), \quad \forall \{\mathbf{u},\mathbf{q},\mathbf{a}\} \in \mathbf{V} \times \mathbf{Q}(\mathbf{u}) \times \mathcal{B}. \tag{7}$$

3.2. Relaxation algorithm

For the solution of (7), we propose a relaxation algorithm of the ADMM-type. Let $\mathbf{m}^0 \in \mathbf{V}$ be a given function (typically the identity function $\mathbf{m}^0(x,y) = (x,y)^T$). Then, for $n \ge 0$:

1. When $\mathbf{m}^n$ is known, we look for

$$\mathbf{b}^{n+1} = \arg\min_{\mathbf{a}\in\mathcal{B}} J_2\left(\mathbf{m}^n, \mathbf{a}\right); \tag{8}$$

2. When $\mathbf{m}^n$ is known, we look for

$$\mathbf{p}^{n+1} = \arg\min_{\mathbf{q}\in\mathbf{Q}(\mathbf{m}^n)} J_1\left(\mathbf{m}^n, \mathbf{q}\right); \tag{9}$$

3. When $\mathbf{p}^{n+1}$ and $\mathbf{b}^{n+1}$ are known, we look for

$$\mathbf{m}^{n+1/2} = \arg\min_{\mathbf{v}\in\mathbf{V}} J\left(\mathbf{v}, \mathbf{p}^{n+1}, \mathbf{b}^{n+1}\right); \tag{10}$$

4. When $\mathbf{m}^{n+1/2}$ is known, we update the solution by

$$\mathbf{m}^{n+1} = \mathbf{m}^n + \omega\left(\mathbf{m}^{n+1/2} - \mathbf{m}^n\right), \tag{11}$$

where $\omega \in (0, 2)$ is a relaxation parameter that helps controlling the convergence speed, and we set $n \to n + 1$.

Looking closely at the relaxation algorithm, we observe that (8) is a local projection problem on the boundary of the domain, which can be solved algebraically. Problem (9) is a local algebraic nonlinear problem, which is reminiscent of those addressed in [8]. Finally, (10) is a global linear variational problem. The solution methods for each of those will be detailed in the following sections.

3.3. Numerical solution of the local boundary projections

Problem (8) can be solved pointwise, as it does not involve any derivatives. It corresponds to solving

$$\min_{\mathbf{b}\in\mathcal{B}} |\mathbf{m}^n(x, y) - \mathbf{b}(x, y)|^2, \quad \forall (x, y) \in \partial\mathcal{X}.$$

Since the approximation $\mathbf{m}^n(x, y)$ does not necessarily belong to $\partial\mathcal{Y}$ for all $(x, y) \in \partial\mathcal{X}$, there is a mismatch with $\mathbf{b}(x, y) \in \partial\mathcal{Y}$. Thus this minimization problem is an L^2-projection of $\mathbf{m}^n(x, y)$ onto $\partial\mathcal{Y}$. Here, the same solution method is adopted as in [18].

3.4. Numerical solution of the local nonlinear problems

We focus here on the solution of (9). Since $\mathbf{m}^n$ is known, the solution $\mathbf{p}^{n+1}$ is obtained by solving the minimization problem

$$\mathbf{p}^{n+1} = \arg \min_{\mathbf{q} \in \mathbf{Q}(\mathbf{m}^n)} \left[\int_{\mathcal{X}} \frac{1}{2} |\mathbf{q}|^2 \, dxdy - \int_{\mathcal{X}} \nabla \mathbf{m}^n : \mathbf{q} dxdy \right]. \tag{12}$$

Problem (12) can be solved pointwise since it does not involve any derivative for the variable $\mathbf{q}$. The solution can be obtained, locally for all $(x, y) \in \mathcal{X}$, as

$$\mathbf{p}^{n+1}(x, y) = \arg \min_{\mathbf{q} \in \mathbf{E}_{(\mathbf{m}^n, x, y)}} \left[\frac{1}{2} |\mathbf{q}|^2 - \mathbf{b} : \mathbf{q} \right], \tag{13}$$

where

$$\mathbf{E}_{(\mathbf{m}^n, x, y)} = \Big\{ \mathbf{q}(x, y) \in \mathbb{R}^{2\times 2}, \quad q_{12} = q_{21}, \\ q_{11}(x, y) q_{22}(x, y) - q_{12}(x, y) q_{21}(x, y) = \frac{f(x, y)}{g(\mathbf{m}^n(x, y))} \Big\},$$

and $\mathbf{b} = \nabla \mathbf{m}^n(x, y)$. Problem (13) is solved with the $\mathbf{Q}_{\min}$ algorithm described in [8, 19], and briefly recalled here.

Setting $\mathbf{p}^{n+1}(x, y) = \mathbf{S}^{n+1}(x, y) \mathbf{\Lambda}^{n+1}(x, y) \mathbf{S}^{n+1}(x, y)^T$, we reformulate (13) as: find $(\mathbf{\Lambda}^{n+1}(x, y), \mathbf{S}^{n+1}(x, y)) \in \mathcal{E}_f(x, y)$ solution of

$$\min_{(\mathbf{\Lambda}, \mathbf{S}) \in \mathcal{E}_f(x,y)} \left[\frac{1}{2} (\mu_1^2 + \mu_2^2) - \text{trace} \left(\mathbf{b} \mathbf{S} \mathbf{\Lambda} \mathbf{S}^T \right) \right], \tag{14}$$

where $\mathcal{E}_f(x, y) = \left\{ (\mathbf{\Lambda}, \mathbf{S}), \, \mathbf{\Lambda} = \text{diag}(\mu_1, \mu_2), \, \mu_1 \mu_2 = \frac{f(x,y)}{g(\mathbf{m}^n(x,y))}, \, \mathbf{S}^T \mathbf{S} = \mathbf{I} \right\}$.

Let $\mathbf{b}' = \mathbf{b} / \sqrt{f(x, y)/g(\mathbf{m}^n(x, y))}$, $\mathbf{M} = \begin{pmatrix} 0 & 1 \\ 1 & 0 \end{pmatrix}$ and $\ell = (\mu_1, \mu_2)^T$ where $\{\mu_1, \mu_2\}$ being the spectrum of $\mathbf{A}$ which belongs to the following set

$$\mathcal{A}_1 = \left\{ \mathbf{A} \in \mathbb{R}^{2\times 2}, \, \mathbf{A} = \mathbf{A}^T, \, \ell^T \mathbf{M} \ell = 2, \, \mathbf{M} \ell \geq 0 \right\}.$$

If we take $\{\lambda_1, \lambda_2\}$ to be the spectrum of $\mathbf{b}'$, then, the constraint $\ell^T \mathbf{M} \ell = 2$ corresponds to $\lambda_1 + \lambda_2 = 1$, and the constraint $\mathbf{M} \ell \geq 0$ ensures that $\lambda_1, \lambda_2 \geq 0$. Further details can be found in [19]. Problem (14) is therefore equivalent to

$$\min_{\mathbf{A} \in \mathcal{A}_1} \text{trace} \left[\mathbf{A} \mathbf{A} - 2 \mathbf{b}' \mathbf{A} \right], \tag{15}$$

which, after some simplification, is reduced to the following one-dimensional equation

$$\frac{\beta_1^2}{(1+\mu)^2} = 2 + \frac{\beta_2^2}{(1-\mu)^2},$$

where $\beta_1 = (\lambda_1 + \lambda_2)/\sqrt{2}$ and $\beta_2^2 = (\lambda_1^2 + \lambda_2^2)/2 - \lambda_1\lambda_2$, which is solved with a Newton algorithm.

3.5. Numerical solution of the linear variational problems

Finding the solution of (10) is equivalent to solving:

$$\min_{\mathbf{v}\in\mathbf{V}} \left\{ \frac{\alpha}{2} \int_{\mathcal{X}} \left|\nabla \mathbf{v} - \mathbf{p}^{n+1}\right|^2 dxdy + \frac{(1-\alpha)}{2} \int_{\partial\mathcal{X}} \left|\mathbf{v} - \mathbf{b}^{n+1}\right|^2 ds \right\}. \tag{16}$$

We derive the first optimality conditions corresponding to (16) and obtain the variational formulation: find $\mathbf{m}^{n+1/2} \in \mathbf{V}$ such that

$$\begin{aligned} \alpha \int_{\mathcal{X}} \nabla \mathbf{m}^{n+1/2} : \nabla \mathbf{v} dxdy + (1-\alpha) \int_{\partial\mathcal{X}} \mathbf{m}^{n+1/2} \cdot \mathbf{v} ds \\ = \alpha \int_{\mathcal{X}} \mathbf{p}^{n+1} : \nabla \mathbf{v} dxdy + (1-\alpha) \int_{\partial\mathcal{X}} \mathbf{b}^{n+1} \cdot \mathbf{v} ds, \end{aligned}$$

for all $\mathbf{v} \in \mathbf{V}$. This weak formulation corresponds to the strong formulation of an elliptic partial differential equation, with Robin boundary conditions: find $\mathbf{m}^{n+1/2} : \mathcal{X} \to \mathbb{R}^2$ such that

$$\begin{aligned} -\alpha \Delta \mathbf{m}^{n+1/2} &= \alpha \mathbf{p}^{n+1} && \text{in } \mathcal{X}, \\ (1-\alpha)\mathbf{m}^{n+1/2} + \alpha \nabla \mathbf{m}^{n+1/2} \cdot \mathbf{n} &= (1-\alpha)\mathbf{b}^{n+1} + \alpha \nabla \cdot \mathbf{p}^{n+1} \cdot \mathbf{n} && \text{on } \partial\mathcal{X}. \end{aligned}$$

Note that the case when $\alpha = 1$ (Neuman boundary conditions) is not well-posed, while the case when $\alpha = 0$ corresponds to the case with Dirichlet boundary conditions. In the numerical experiments hereafter, we take $\alpha = 1/2$.

4. Finite element approximation

Let $h > 0$ be a space discretization step and let $\mathcal{T}_h$ be a discretization of $\mathcal{X}$. Let $\mathcal{X}_h$ be the discretized version of $\mathcal{X}$; for the sake of simplicity of the notation, let us assume that $\mathcal{X}_h \equiv \mathcal{X}$. Let $\mathbf{Q}_h$ be the space defined as

$$\mathbf{Q}_h = \left\{ \mathbf{q} \in L^2\left(\mathcal{X}_h\right)^{2\times 2},\ \mathbf{q}|_T \in \mathbb{R}^{2\times 2},\ \forall T \in \mathcal{T}_h \right\},$$

equipped with the discrete inner product and corresponding norm:

$$((\mathbf{p},\mathbf{q}))_{0h} = \sum_{T\in\mathcal{T}_h} |T|\ \mathbf{p}|_T : \mathbf{q}|_T\,, \qquad |||\mathbf{q}|||_{0h} = \sqrt{((\mathbf{q},\mathbf{q}))_{0h}}.$$

Let $\mathbf{Q}_{f,g,\mathbf{m}_h,h}$ be the finite dimensional subset approximating $\mathbf{Q}(\mathbf{m})$ and defined by

$$\mathbf{Q}_{f,g,\mathbf{m}_h,h} = \left\{ \mathbf{q}\in\mathbf{Q}_h,\ \mathbf{q}=\mathbf{q}^T,\ \det\mathbf{q}|_T = \left[\overline{\frac{f}{g(\mathbf{m}_h)}}\right]_T,\ \forall T\in\mathcal{T}_h \right\},$$

where $\left[\overline{F}\right]_T$ denotes the average of the generic quantity F over a generic element T. Let $\mathbf{V}_h$ be the finite dimensional subspace of $\mathbf{V}$ given by continuous piecewise linear finite elements:

$$\mathbf{V}_h = \left\{ \mathbf{v}\in\left(C^0\left(\overline{\mathcal{X}_h}\right)\right)^2,\ \mathbf{v}|_T\in(\mathbb{P}_1)^2,\ \forall T\in\mathcal{T}_h \right\},$$

where $\mathbb{P}_1$ is the space of the two-variable polynomials of degree ≤ 1. We define a discrete inner product and the corresponding norm for $\mathbf{V}_h$ as

$$(\mathbf{u},\mathbf{v})_{0h} = \sum_{T\in\mathcal{T}_h}\sum_{i=1}^{m} W_i\mathbf{u}(\zeta_i)\cdot\mathbf{v}(\zeta_i)\,, \qquad \|\mathbf{u}\|_{0h} = \sqrt{(\mathbf{u},\mathbf{u})_{0h}}\,,$$

with W_i the weights and ζ_i the evaluation points of a Gauss quadrature rule, m denoting the number of points of the quadrature rule. Finally, let us consider a sequence of successive points $\mathbf{y}_i\in\partial\mathcal{Y}$, with $\mathbf{y}_0=\mathbf{y}_{N+1}$ (to form a closed loop). The piecewise linear approximation of $\partial\mathcal{Y}_h$ is defined by the union of segments

$$\partial\mathcal{Y}_h = \bigcup_{i=0}^{N}[\mathbf{y}_i,\mathbf{y}_{i+1}].$$

Let $\mathcal{B}_h$ be the finite dimensional subspace of $\mathcal{B}$ defined as:

$$\mathcal{B}_h = \left\{ \mathbf{b}\in\left(C\left(\partial\mathcal{X}_h\right)\right)^2, \mathbf{b}|_{[\mathbf{y}_i,\mathbf{y}_{i+1}]}\in(\mathbb{P}_1)^2,\ \forall i=0,\ldots,N \right\}. \tag{17}$$

The discrete formulation of the least-squares method to solve (7) reads as follows: find $\{\mathbf{m}_h,\mathbf{p}_h,\mathbf{b}_h\}\in\mathbf{V}_h\times\ \mathbf{Q}_{f,g,\mathbf{m}_h,h}\times\ \mathcal{B}_h$ such that

$$J(\mathbf{m}_h,\mathbf{p}_h,\mathbf{b}_h)\leq J(\mathbf{u}_h,\mathbf{q}_h,\mathbf{a}_h)\,,\ \ \forall\{\mathbf{u}_h,\mathbf{q}_h,\mathbf{a}_h\}\in\mathbf{V}_h\times\mathbf{Q}_{f,g,\mathbf{u}_h,h}\times\mathcal{B}_h. \tag{18}$$

The discrete formulation of the relaxation algorithm (8)–(11) becomes the following: we initialize first the algorithm with $\mathbf{m}_h^0 \in \mathbf{V}_h$. Then, for $n \geq 0$,

1. We solve the projection problem

$$\mathbf{b}_h^{n+1} = \mathbb{P}_{\mathcal{Y}_h}(\mathbf{m}_h^n),$$

where $\mathbb{P}_{\mathcal{Y}_h}(\cdot)$ is the orthogonal projection operator on the discrete boundary $\partial\mathcal{Y}_h$ described, e.g., in [18].

2. We solve the discrete local nonlinear problem:

$$\mathbf{p}_h^{n+1} = \arg \min_{\mathbf{q}_h \in \mathbf{Q}_{f,g,\mathbf{m}_h^n,h}} \left[((\mathbf{q}_h, \mathbf{q}_h))_{0h}^2 - ((\nabla \mathbf{m}_h^n, \mathbf{q}))_{0h} \right]. \tag{19}$$

The solution of the discrete minimization problem (19), $\mathbf{p}_h^{n+1}$, is obtained using the algorithm $\mathbf{Q}_{\min}$ on each element T of $\mathcal{T}_h$, in an identical manner as the solution of the continuous problem described in Section 3.4.

3. We solve the discrete linear variational problem:

$$\min_{\mathbf{v}_h \in \mathbf{V}_h} \left\{ \frac{\alpha}{2} \left| \left| \left| \nabla \mathbf{v}_h - \mathbf{p}_h^{n+1} \right| \right| \right|_{0h}^2 + \frac{(1-\alpha)}{2} \int_{\partial\mathcal{X}_h} \left| \mathbf{v}_h - \mathbf{b}_h^{n+1} \right|^2 ds \right\}. \tag{20}$$

We derive the first optimality conditions corresponding to (20) and obtain the, finite element based, variational formulation: find $\mathbf{m}_h^{n+1/2} \in \mathbf{V}_h$ such that

$$\begin{aligned} &\alpha \left(\left(\nabla \mathbf{m}_h^{n+1/2}, \nabla \mathbf{v}_h \right) \right)_{0,h} + (1-\alpha) \int_{\partial\mathcal{X}_h} \mathbf{m}_h^{n+1/2} \cdot \mathbf{v}_h ds \\ &\quad = \alpha \left(\left(\mathbf{p}_h^{n+1}, \nabla \mathbf{v}_h \right) \right)_{0,h} + (1-\alpha) \int_{\partial\mathcal{X}_h} \mathbf{b}_h^{n+1} \cdot \mathbf{v}_h ds, \end{aligned}$$

for all $\mathbf{v}_h \in \mathbf{V}_h$.

4. We update the solution with $\mathbf{m}_h^{n+1} = \mathbf{m}_h^n + \omega \left(\mathbf{m}_h^{n+1/2} - \mathbf{m}_h^n \right)$.

5. Numerical experiments

Numerical experiments are presented in order to validate the convergence and accuracy properties of the least-squares methodology. For computational domains, we consider square and disk domains. Typical triangulations of these domains are illustrated in Figure 2. The relaxation parameter ω is set

to approx. 1 initially, and then is increased to $\omega = 2$. The stopping criterion for the relaxation algorithm is $\|\mathbf{m}_h^n - \mathbf{m}_h^{n-1}\|_{0h} < 10^{-8}$. The parameter α is set to $\alpha = 0.5$.

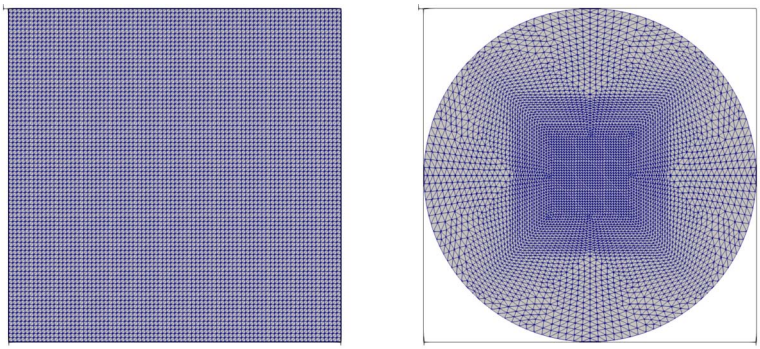

Figure 2: Typical finite element meshes used for the numerical experiments. Left: structured mesh for a square domain ($h = 0.0125$); Right: structured mesh for the unit disk domain ($h \simeq 0.0209$).

In order to accelerate the performance of our algorithm, the gradients are post-processed with a gradient reconstruction procedure. More specifically, for any $\mathbf{v}_h \in \mathbf{V}_h$, and for any vertex P of the finite element triangulation:

$$\frac{\partial \mathbf{v}_h}{\partial x_i}(P) := \frac{\displaystyle\sum_{T \in \mathcal{T}_h, P \in T} |T| \left.\frac{\partial \mathbf{v}_h}{\partial x_i}\right|_T}{\displaystyle\sum_{T \in \mathcal{T}_h, P \in T} |T|}, \qquad i = 1, 2.$$

5.1. Validation test case: identity map

First, we consider the test case for which the exact solution is the identity map when $\mathcal{X} \equiv \mathcal{Y}$. The source and target functions are selected as $f = 1$ and $g = 1$. The exact solution is $\mathbf{m}(x, y) = (x, y)^T$.

Table 1 illustrates the convergence order of the method in the $L^2(\Omega)$ and $H^1(\Omega)$ norms, and shows convergence with order one for both. Moreover, $\|\nabla \mathbf{m}_h - \mathbf{p}_h\|_{L^2(\Omega)}$ also decreases with order one as the mesh size h is reduced.

5.2. Transport of a circle to an ellipse

Let us consider a test for which $\mathcal{X} \neq \mathcal{Y}$ are both enclosed into a sufficiently large domain Ω. Let us consider $\Omega = (-4, 4) \times (-2, 2)$. In this test case we

Table 1: Validation test case: Identity map. Computational results for several mesh sizes h. The columns describe the L^2- and H^1-norms of the error, rates of convergence, norm of the residual, and number of relaxation algorithm iterations

h	$\|\mathbf{m}-\mathbf{m}_h\|_{L^2(\Omega)}$		$\|\mathbf{m}-\mathbf{m}_h\|_{H^1(\Omega)}$		$\|\nabla\mathbf{m}_h-\mathbf{p}_h\|_{L^2(\Omega)}$	iter
0.100	2.22e-02		3.75e-02		3.71e-02	69
0.0500	1.12e-02	0.98	1.92e-02	0.89	1.88e-02	69
0.0250	5.70e-03	0.97	9.71e-03	0.98	9.51e-03	69
0.0125	2.87e-03	0.97	4.89e-03	0.99	4.79e-03	69

map the unit circle

$$\mathcal{X} = \left\{(x,y) \in \Omega \ : \ x^2+y^2 < 1\right\},$$

into the ellipse domain

$$\mathcal{Y} = \left\{(x,y) \in \Omega \ : \ \frac{(x-2)^2}{2^2} + \frac{y^2}{0.5^2} < 0.25\right\}.$$

The domain $\mathcal{X}$ is equipped with finite element triangulations such as those illustrated in Figure 2. We consider $f = 1$ and $g = 1$ defined on $\mathcal{X}$ and $\mathcal{Y}$ respectively. An exact solution of this map is given by $\mathbf{m}(x,y) = (2x+2, 0.5y)^T$.

Figure 3 illustrates the optimal transport from the source domain $\mathcal{X}$ (left) into the target domain $\mathcal{Y}$ (right). One can observe that the symmetry of the original mesh points is conserved after transport. Table 2 illustrates the convergence orders in the $L^2(\mathcal{X})$ and $H^1(\mathcal{X})$ norms. Both norms show again convergence with order (actually better than) one, which is appropriate for mixed piecewise linear finite elements. Similarly, $\|\nabla\mathbf{u}_h-\mathbf{p}_h\|_{L^2(\mathcal{X})}$ also shows an order one convergence order.

Table 2: Transport of a circle to an ellipse. Computational results for several mesh sizes h. The columns describe the L^2- and H^1-norms of the error, rates of convergence, norm of the residual, and number of relaxation algorithm iterations

h	$\|\mathbf{m}-\mathbf{m}_h\|_{L^2(\mathcal{X})}$		$\|\mathbf{m}-\mathbf{m}_h\|_{H^1(\mathcal{X})}$		$\|\nabla\mathbf{m}_h-\mathbf{p}_h\|_{L^2(\mathcal{X})}$	iter
0.0831	9.08e-01		1.16e+00		2.01e-01	859
0.0416	3.31e-01	1.45	5.62e-01	1.04	1.02e-01	609
0.0208	1.20e-01	1.46	2.60e-01	1.11	5.57e-02	499
0.0104	6.09e-02	1.46	1.40e-01	0.89	2.94e-02	449

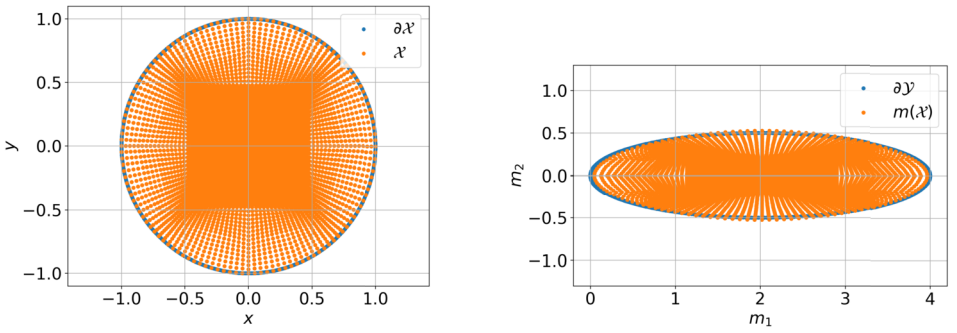

Figure 3: Transport of a circle to an ellipse. Snapshots of the supports of the original and final density functions. The results are obtained on structured mesh of the unit disk with $h = 0.0209$.

5.3. Transport of a Gaussian to a Gaussian

We consider the optimal transportation of a Gaussian density onto another Gaussian density. Let us recall that the probability distribution of a generic Gaussian density reads as follows:

$$\psi_{(x_0,y_0),\sigma}(x,y) = \frac{2}{\sigma\sqrt{2\pi}} \exp\left(-\frac{1}{2}\frac{(x-x_0)^2+(y-y_0)^2}{\sigma^2}\right),$$

where (x_0, y_0) is the center, and σ the strandard deviation. Here we analyze the scenario where the source function is f is $f(x,y) = \psi_{(-0.7,-0.7),0.2}(x,y)$ and the target function is $g(x,y) = \psi_{(0.7,0.7),0.2}(x,y)$. The domain $\mathcal{X}$ is defined in $(-2,2)^2$ and $\partial\mathcal{Y} = \partial\mathcal{X}$. For this numerical experiment, the exact solution is not known.

In order to help the convergence of the algorithm and safeguard it, we practically replace the right hand side of (6) by a regularized version:

$$\frac{f(x,y)}{g(\mathbf{m}(x,y))} \to \max\left(\frac{\varepsilon + f(x,y)}{\varepsilon + g(\mathbf{m}(x,y))}, 10\right),$$

where, in the experiments, $\varepsilon = 10^{-5}$. This regularization helps to control the ratio of the source and target functions, ensuring that it does not lead to instabilities in our algorithm, while not affecting the expected solution. We consider a single numerical experiment with a step size $h = 0.025$ and a maximum of 2,500 iterations. Based on these preliminary results, we can make the following remarks:

- The L^2 norm of the residual $\|\nabla \mathbf{m}_h - \mathbf{p}_h\|_{L^2(\mathcal{X})}$, is approximately 1.625. This quantity measures the difference between the solutions of the linear and the non-linear problems.
- The residual of the equation $\|\det \nabla \mathbf{m}(x,y) - \frac{f(x,y)}{g(\mathbf{m}(x,y))}\|_{L^2(\mathcal{X})}$ is approximately 4.4567.
- The integrals of the source and target densities over $\mathcal{X}$, given by $\int_{\mathcal{X}} f(x,y)dxdy$ and $\int_{\mathcal{X}} g(x,y)dxdy$, are both equal to 1 by definition. However, the integral of the transformed target density over $\mathcal{X}$, computed as $\int_{\mathcal{X}} g(\mathbf{m}(x,y))$, is 0.77, suggesting a loss in density during the transport.
- On the other hand, the peak amplitude of the source function $f(x,y)$ is 3.98943 at $(-0.7,-0.7)$, while that of the transformed target function $g(\mathbf{m}(x,y))$ is 3.98531 at $(-0.65,-0.65)$. This suggests that peak amplitude was preserved while the position of the peak shifts slightly. This effect highlights the fact that the transport may have to be solved in smaller steps (see, e.g., [15]).
- The L^2 norm of the difference between the source density and the transformed target density, denoted as $\|f(x,y) - g(\mathbf{m}(x,y))\|_{L^2(\mathcal{X})}$, is 0.53.

Figure 4 shows the source function $f(x,y)$ and the target density $g(\mathbf{m}(x,y))$ after a partial shift. Figure 5 illustrates the numerical approximation of each component of $\mathbf{m}$.

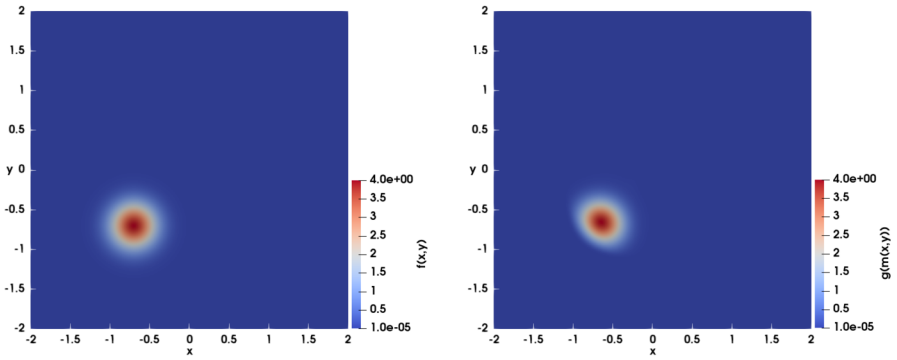

Figure 4: Transport of a Gaussian to another Gaussian. Left: source function $f(x,y)$; Right: transported density $g(\mathbf{m}(x,y))$. The results are obtained using a structured mesh of the square domain with a grid size of $h = 0.025$.

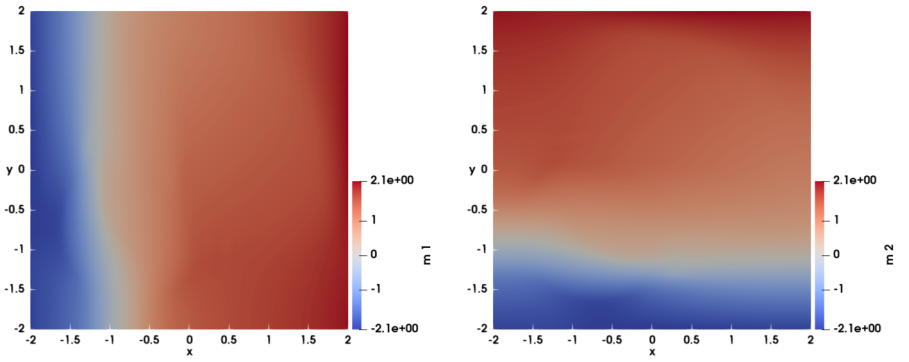

Figure 5: Transport of a Gaussian to another Gaussian. Snapshots of the first component (left) and the second component (right) of the numerical approximation of $\mathbf{m}$. The results are obtained using a structured mesh of the square domain with a grid size of $h = 0.025$.

6. Conclusions

A numerical method based on a least-squares approach has been presented to solve an optimal transport problem in two dimensional space. Inspired from [18], the framework includes a combination of several algorithms inspired from previous works [6, 7], in particular the $\mathbf{Q}_{\min}$ algorithm [8].

Numerical results in simple situations have highlighted the appropriate convergence order of the method, and even super-convergence in some cases. Numerical experiments have also illustrated the need to investigate further iterative approaches for transport to avoid numerical diffusion, for instance when including Gaussian densities. Perspectives include the incorporation of non-convex cost functions to model obstacles, and the incorporation of several sources and destinations for real-life applications.

Acknowledgements

The authors thank Prof. Marco Picasso (EPFL) and Giulia Lécureux (HEG) for fruitful discussions.

References

[1] Ambrosio, L., Caffarelli, L. A., Brenier, Y., Buttazzo, G., Villani, C. and Salsa, S. (2003). *Optimal Transportation and Applications*. Springer Berlin, Heidelberg. MR2006302

[2] Benamou, J., Froese, B. D. and Oberman, A. M. (2014). Numerical solution of the Optimal Transportation problem using the Monge-Ampère equation. *Journal of Computational Physics* **260** 107–126. MR3151832

[3] Benamou, J. D. and Brenier, Y. (2000). A computational fluid mechanics solution to the Monge-Kantorovich mass transfer problem. *Numerische Mathematik* **84** 375–393. MR1738163

[4] Benamou, J. D., Froese, B. D. and Oberman, A. M. (2010). Two numerical methods for the elliptic Monge-Ampère equation. *ESAIM: Mathematical Modelling and Numerical Analysis* **44** 737–758. MR2683581

[5] Bottani, E., Mannino, F., Vignali, G. and Montanari, R. (2018). A routing and location model for food waste recovery in the retail and distribution phase. *International Journal of Logistics Research and Applications* **21** 557–578.

[6] Caboussat, A. and Glowinski, R. (2018). An alternating direction method of multipliers for the numerical solution of a fully nonlinear partial differential equation involving the Jacobian determinant. *SIAM Journal on Scientific Computing* **40** A52–A80. MR3742695

[7] Caboussat, A., Glowinski, R. and Gourzoulidis, D. (2022). A least-squares / relaxation method for the numerical solution of a partial differential equation involving the Jacobian determinant. *Journal of Scientific Computing* **93** 1–32. MR4475302

[8] Caboussat, A., Glowinski, R. and Sorensen, D. C. (2013). A least-squares method for the numerical solution of the Dirichlet problem for the elliptic Monge-Ampère equation in dimension two. *ESAIM: Control, Optimization and Calculus of Variations* **19** 780–810. MR3092362

[9] Caffarelli, L. A. and Cabré, X. (1995). *Fully Nonlinear Elliptic Equations*. American Mathematical Society. MR1351007

[10] Dacorogna, B. and Moser, J. (1990). On a partial differential equation involving the Jacobian determinant. *Annales de l'I.H.P. Analyse non Linéaire* **7** 1–26. MR1046081

[11] Figalli, A. (2017). *The Monge-Ampère Equation and Its Applications. Zurich Lectures in Advanced Mathematics*. European Mathematical Society. MR3617963

[12] Lakkis, O. and Pryer, T. (2013). A finite element method for fully nonlinear elliptic problems. *SIAM Journal on Scientific Computing* **35** A2025–A2045. MR3085125

[13] Monge, G. (1781). Mémoire sur la théorie des déblais et des remblais. *Histoire de l'Académie Royale des Sciences avec les Mémoires de Mathématique et de Physique tirés des Registres de cette Académie* 666–705.

[14] Oberman, A. M. and Ruan, Y. (2015). An efficient linear programming method for Optimal Transportation.

[15] Papadakis, N., Peyré, G. and Oudet, E. (2014). Optimal transport with proximal splitting. *SIAM Journal on Imaging Sciences* **7** 212–238. MR3158785

[16] Peyré, G. and Cuturi, M. (2017). Computational optimal transport. *Center for Research in Economics and Statistics. Working Papers* **2017-86**.

[17] Philippis, G. D. and Figalli, A. (2014). The Monge-Ampère equation and its link to optimal transportation. *Bulletin of the American Mathematical Society* **51** 527–580. MR3237759

[18] Prins, C. R., Beltman, R., Thije ten Boonkkamp, J. H. M., Ijzerman, W. L. and Tukker, T. W. (2015). A least-squares method for optimal transport using the Monge-Ampère equation. *SIAM Journal on Scientific Computing* **37** B937–B961. MR3427051

[19] Sorensen, D. C. and Glowinski, R. (2010). A quadratically constrained minimization problem arising from PDE of Monge-Ampère type. *Numerical Algorithms* **53** 53–66. MR2566127

[20] Vanderbei, R. J. (2020). *Linear Programming*. Springer. MR2363558

[21] Villani, C. (2003). *Topics in Optimal Transportation*. American Mathematical Society, USA. MR1964483

[22] Yadav, N. K., Thije ten Boonkkamp, J. H. M. and Ijzerman, W. L. (2019). A Monge-Ampère problem with non-quadratic cost function to compute freeform lens surfaces. *Journal of Scientific Computing* **80** 475–499. MR3954451

Alexandre Caboussat
Geneva School of Business Administration (HEG)
University of Applied Sciences Western Switzerland (HES-SO)
Rue de la Tambourine 17
1227 Carouge
Switzerland
E-mail address: alexandre.caboussat@hesge.ch

Dimitrios Gourzoulidis
Geneva School of Business Administration (HEG)
University of Applied Sciences Western Switzerland (HES-SO)
Rue de la Tambourine 17
1227 Carouge
Switzerland
E-mail address: dimitrios.gourzoulidis@hesge.ch

Received July 31, 2023